

Construct	Dose-Response Curve Properties				
	Leakiness	Fold Change	EC50	Hill Slope	Area
LLL	3.2 ± 0.01	31.5 ± 0.36	4.54E-09	1.15	150800
LLT		32.5 ± 0.12	1.1E-8	0.78	144340
LLA		29.3 ± 0.03	4.75E-7	0.62	81113
LLR		1.3 ± 0.01	–	–	180
LAL	2.08 ± 0.02	3.6 ± 0.45	≥5E-5	–	644
LAT		26.9 ± 0.26	2.08E-06	1.13	35200
LAA		28.6 ± 0.42	1.34E-08	0.69	83782
LAR		2.5 ± 0.28	≥5E-5	–	425
LRL	2.52 ± 0.01	3.1 ± 0.40	≥5E-5	–	402
LRT		2.7 ± 0.07	≥5E-5	–	546
LRA		1.1 ± 0.01	–	–	18
LRR		29.9 ± 0.22	1.37E-09	1.14	131890
TTL	1.74 ± 0.01	5.1 ± 0.06	5.89E-08	1.01	8235
TTT		5.4 ± 0.06	3.16E-08	1.19	9390
TTA		7.1 ± 0.05	9.65E-7	0.86	8067
TTR		1.1 ± 0.01	–	–	43
AAL	3.93 ± 0.01	15.4 ± 2.35	≥5E-5	–	5003
AAT		90.3 ± 0.52	5.95E-7	1.29	279910
AAA		98.7 ± 1.11	1.18E-09	0.94	689740
AAR		8.1 ± 1.55	≥5E-5	–	2639
RLL	2.40 ± 0.01	64.5 ± 0.51	3.15E-7	0.45	156500
RLT		63.0 ± 0.17	2.57E-06	0.41	122680
RLA		19.6 ± 0.16	2.00E-03	0.41	20147
RLR		1.0 ± 0.0	–	–	53
RAL	2.28 ± 0.04	6.6 ± 0.94	≥5E-5	–	1223
RAT		59.8 ± 0.43	1.03E-06	1.12	93241
RAA		62.6 ± 1.45	8.39E-10	0.58	241590
RAR		3.7 ± 0.54	≥5E-5	–	641
RRL	5.71 ± 0.07	7.0 ± 0.73	≥5E-5	–	3551
RRT		6.7 ± 0.11	≥5E-5	–	3839
RRA		1.9 ± 0.20	≥5E-5	–	1036
RRR		27.7 ± 0.12	4.99E-10	1.299	306560

Table S1 Characteristics of QS circuit dose-responses. Each promoter-R-protein pair has the same leakiness regardless of HSL, so it is only listed once. EC50 was not estimated for constructs with fold changes lower than 2, and any construct that exhibited a greater than 2-fold change only at 100uM was assumed to have an EC50 greater than or equal to 50uM. Hill slopes were only calculated for constructs that showed significant activation before 100uM.

Name	Sequence	Organism	Reference
Plux	ACTATTGTATCGCTGGGAATACAATTACTTAAACATAAGCAC CTGTAGGATCGTACAGGTTT TACGCAAGAAAATGGTTTGT ATAGTCGAATAT	Aliivibrio fischeri	(Hasty Lab)
Ptra (pCF370)	CTACGTGCAGATCTGCACAT AGCCACACCCTGAATGAGATG TTTTCTCTCCGCTA	Agrobacterium tumefaciens	(54) White 2007, (53) Fuqua 1996
Plas	TTCGAGCCTAGCAAGGGTCCGGGTTACCGAAA TCTATCTC ATTTGCTAGTT TATAAAATTATGAAATTTGCGTAAATTTCTT CA	Pseudomonas aeruginosa	(Hasty Lab)
Prpa	ACCTGTCCGATCGGACAGT AGTTAGGTTCCCGTTCGCACCT GCACTGTTCCCGCCTGCA	Rhodopseudomonas palustris	(56) Hirakawa 2011
Pahy	ACCGAAGTGAAATGTTTCGAGGTA CTCAAGCAGTTGGTCTTG TTTCATATGCTAGCCCCCTGGCCAGGGCCTCGATTATA	Aeromonas hydrophila	(61) Garde 2010
Psma	ATAATCTTGT CATGGGTTTTAAATTTACTTGT CACATAGGC TCTGATACA TTACTCGCCG	Serratia marcescens	(62) Slater 2003
Prhl (qscrh1A)	TCCTGTGAAATCTGGCAGTT ACCGTTAGCTTTTCGAATTGG CTAAAAAGTGTTTC	Pseudomonas aeruginosa	(63) Karig 2005
Pcer (PopgG)	GCTGGACGATGCGAATCTTGGAA TTGCGCTCTGCAAGCCAT TGAAAAACGGACGTCGTCTCTGATATGCCCGCTCCTGCCG CCCCCTCCGCCCGCCTGAACCGGGCCTGCTGCTCAGCGCGG CAAGTTCGTGCTCGCCCTCGCTGCAAGCGGGCTC	Rhodobacter sphaeroides	(59) Puskas 1997
Pexp (PwgeA)	TGCCTGCATTT CCGTCAGAATTACTCCTAAAATTATATTG TACCAATAT TGGCACAGCATGGAGATATGTTTCGGGCACCC TCTTTCTATCAAAATATCGCCGTTTTATTTTATGCATCTGTG TTGCGTTCGTAATTATTGCAGTGCACACTCCGGCAGC	Sinorhizobium meliloti	(60) Charoenpanich 2013
Ptra*	GCACGTGCAGATCTGCACAT TTACGCAAGAAAATGGTTTGT TTATAGTCGAATAT	Synthetic	This Study
Prpa*	GCACCTGTCCGATCGGACAGT ATTACGCAAGAAAATGGTT TGTTATAGTCGAATAT	Synthetic	This Study

Table S2 Promoter sequences used in this study. Palindromic lux-box-like receptor-binding sequences in boldface when known.

Plasmid	Genotype	Vector
Bsrs079-LuxR	R6K; Spec; 5' Insulation Unit; BCD7; LuxR-GFP; 3' Insulation Unit	pBjk2807
Bsrs079-LasR	R6K; Spec; 5' Insulation Unit; BCD7; LasR-GFP; 3' Insulation Unit	pBjk2807
Bsrs079-TraR	R6K; Spec; 5' Insulation Unit; BCD7; TraR-GFP; 3' Insulation Unit	pBjk2807
Bsrs079-RpaR	R6K; Spec; 5' Insulation Unit; BCD7; RpaR-GFP; 3' Insulation Unit	pBjk2807
Bsrs079-RhlR	R6K; Spec; 5' Insulation Unit; BCD7; RhlR-GFP; 3' Insulation Unit	pBjk2807
Bsrs079-SinR	R6K; Spec; 5' Insulation Unit; BCD7; SinR-GFP; 3' Insulation Unit	pBjk2807
Bsrs079-CerR	R6K; Spec; 5' Insulation Unit; BCD7; CerR-GFP; 3' Insulation Unit	pBjk2807
Bsrs079-SmaR	R6K; Spec; 5' Insulation Unit; BCD7; SmaR-GFP; 3' Insulation Unit	pBjk2807
Bsrs079-AhyR	R6K; Spec; 5' Insulation Unit; BCD7; AhyR-GFP; 3' Insulation Unit	pBjk2807
Bsrs078-LuxR	R6K; Spec; 5' Insulation Unit; BCD7; LuxR; 3' Insulation Unit	pBjk2807
Bsrs078-TraR	R6K; Spec; 5' Insulation Unit; BCD7; TraR; 3' Insulation Unit	pBjk2807
Bsrs078-TraR(W)	R6K; Spec; 5' Insulation Unit; BCD7; TraR(W); 3' Insulation Unit	pBjk2807
Bsrs078-LasR	R6K; Spec; 5' Insulation Unit; BCD7; LasR; 3' Insulation Unit	pBjk2807
Bsrs078-RpaR	R6K; Spec; 5' Insulation Unit; BCD7; RpaR; 3' Insulation Unit	pBjk2807
Bsrs074-Plux	ColE2; AmpR; Plux; u6; sfGFP	pBjk2992
Bsrs074-Ptra	ColE2; AmpR; Ptra; u6; sfGFP	pBjk2992
Bsrs074-Ptra*	ColE2; AmpR; Ptra*; u6; sfGFP	pBjk2992
Bsrs074-Plas	ColE2; AmpR; Plas; u6; sfGFP	pBjk2992
Bsrs074-Prpa	ColE2; AmpR; Prpa; u6; sfGFP	pBjk2992
Bsrs074-Prpa*	ColE2; AmpR; Prpa*; u6; sfGFP	pBjk2992
Bsrs074-Pahy	ColE2; AmpR; Pahy; u6; sfGFP	pBjk2992
Bsrs074-Psma	ColE2; AmpR; Psma; u6; sfGFP	pBjk2992
Bsrs074-Prhl	ColE2; AmpR; Prhl; u6; sfGFP	pBjk2992
Bsrs074-Pcer	ColE2; AmpR; Pcer; u6; sfGFP	pBjk2992
Bsrs074-Pexp	ColE2; AmpR; Pexp; u6; sfGFP	pBjk2992
Bsrs074-Plux-mKate2	ColE2; Cm; Plux; u6; mKate2	pBjk2992
Bsrs074-Plas-mKate2	ColE2; Cm; Plas; u6; mKate2	pBjk2992
pZA35-Bsrs074-Plux-tra	P15A; Cm; Ptra; u6; sfGFP	pZA35
Bsrs112-TraR-RpaR	R6K; Spec; 5' Insulation Unit; BCD7; TraR(W); mevB-rbs; RpaR; 3' Insulation Unit	pBjk2807
Bsrs112-TraR-LasR	R6K; Spec; 5' Insulation Unit; BCD7; TraR(W); mevB-rbs; LasR; 3' Insulation Unit	pBjk2807
Bsrs103-RpaR-Rpal	ColE1; Kan; RpaR; PluxI; Rpal; T1	pTD103
Bsrs103-RpaR-Lasl	ColE1; Kan; RpaR; PluxI; LasI; T1	pTD103

Table S3 Plasmids used in this study. All constructs were expressed in *E. coli* DIAL Strain “EK” cells.

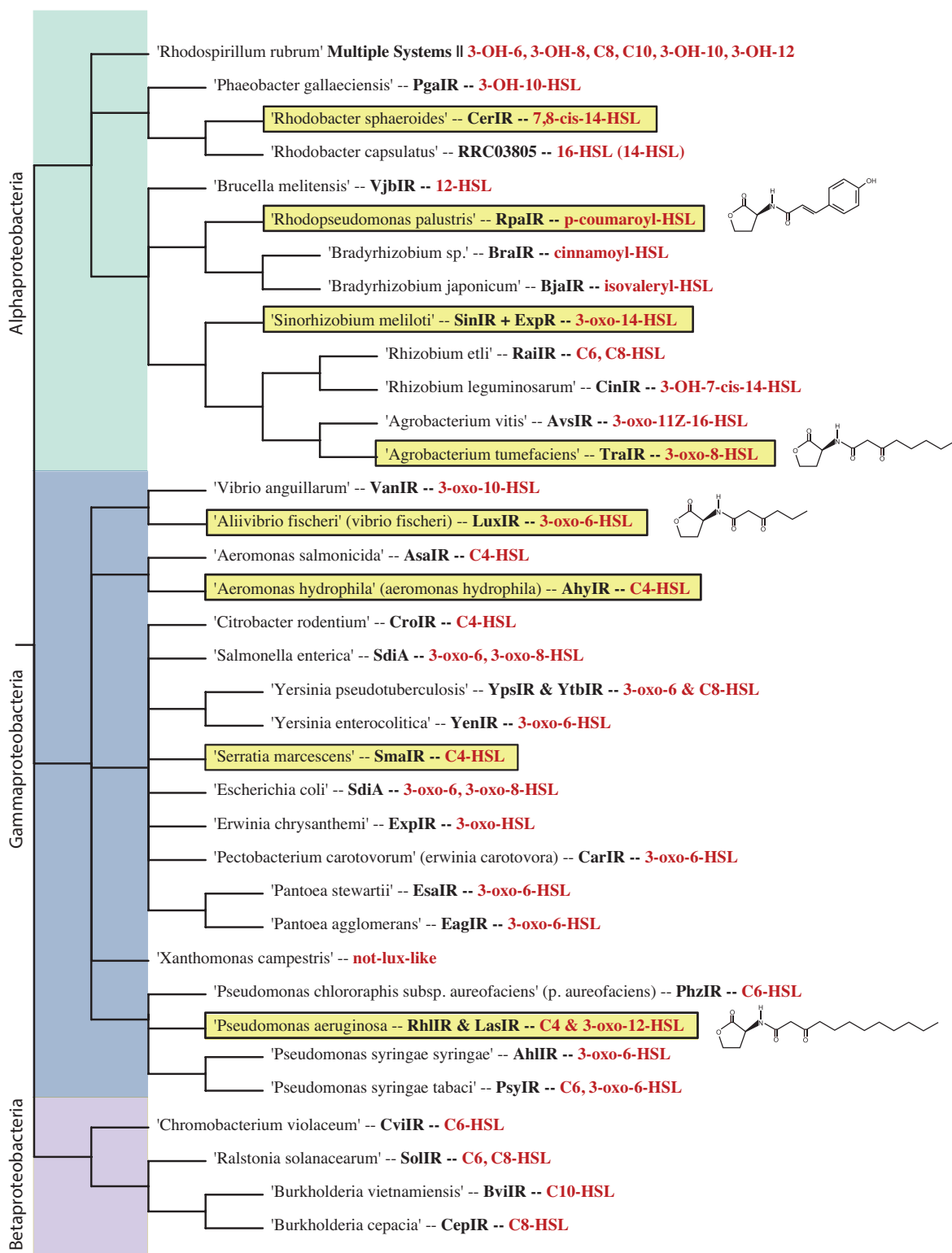


Fig. S1 Evolutionary tree of selected Lux-like QS systems. Systems selected for initial analysis are highlighted in yellow. Each system's HSL is written in red; the chemical structure of the four HSL's particular to the systems characterized in this study are shown on the far right. Potential systems were chosen based on evolutionary distance, ligand uniqueness, and available information in the literature on their potential for recombinant expression

Promoter-Receptor Pair Leakiness

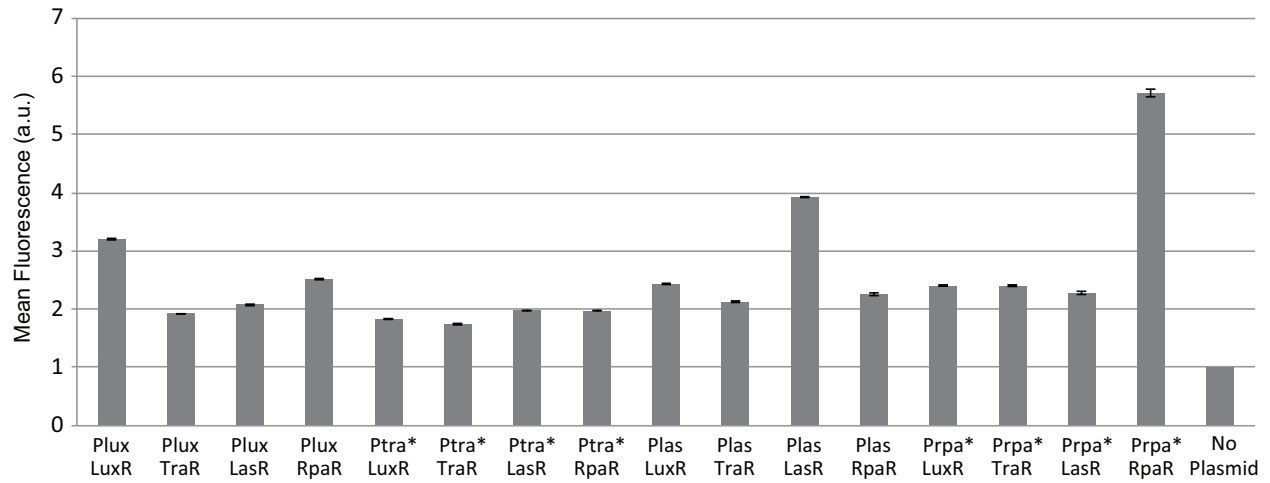


Fig. S2 Promoter/Receptor Pairs Exhibit Differential Basal Expression Levels. Mean fluorescence of Receptor/Reporter two-plasmid systems in the absence of any HSL signal. All values are normalized by the auto-fluorescence of the same *E. coli* strain with no GFP plasmid. Error bars represent S.E.M (n=3).

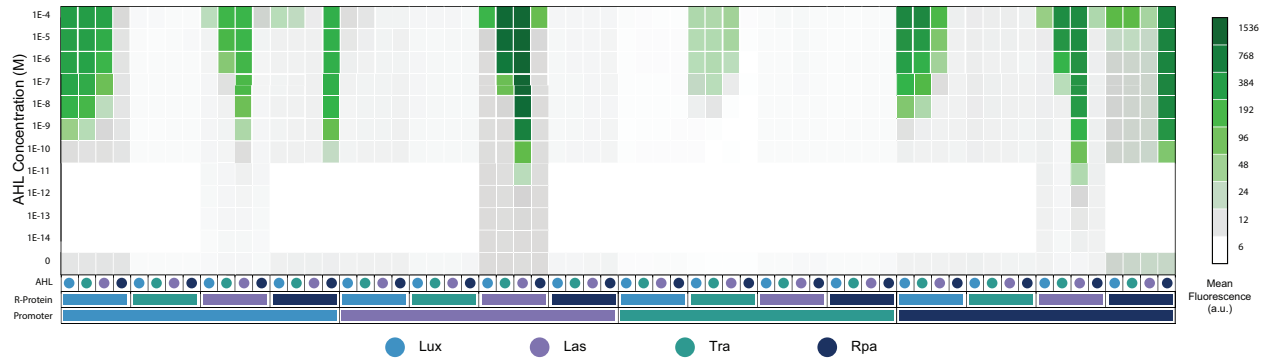


Fig. S3 Heat map showing GFP abundance for all QS combinations and HSL concentrations. Each column denotes a unique combination of signal (HSL), receptor (R- protein), and reporter (QS promoter), with rows denoting the concentration of ligand. Each value corresponds to the mean fluorescence value measured from a cell population normalized by the population's cell-density; all combinations and concentrations were done in triplicate.

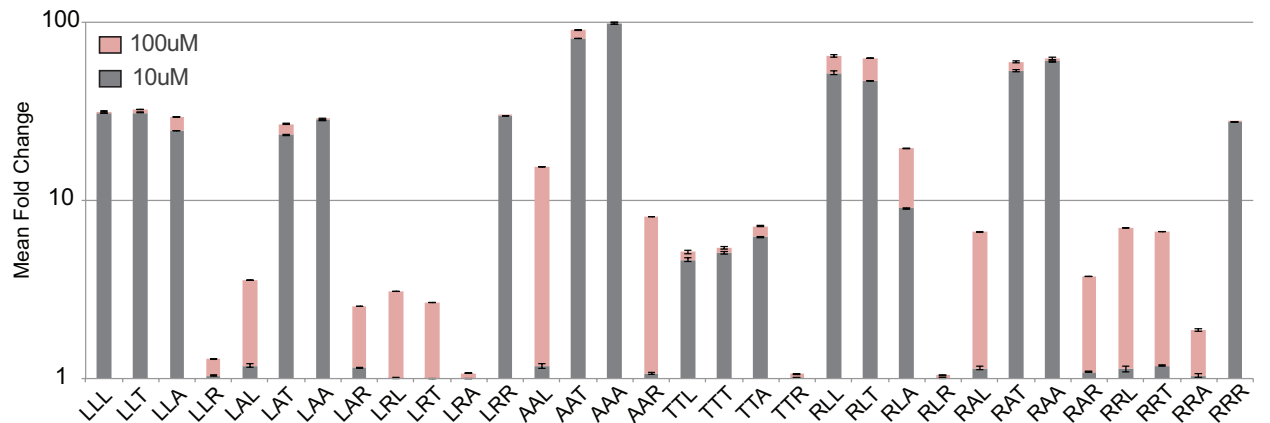


Fig. S4 Large Increase in Expression at 100uM Distorts Relative Performance of Constructs. Fluorescence value at 10uM and 100uM divided by basal expression rate in absence of HSL to give Fold Change, error bars denote SEM (n=3). Many systems still show little to no expression at the already very high ligand concentration of 10uM, but exhibit a large jump in expression at 100uM. Since this concentration value is thought to be physiologically irrelevant, fold change based off that concentration can inaccurately describe promoter performance.

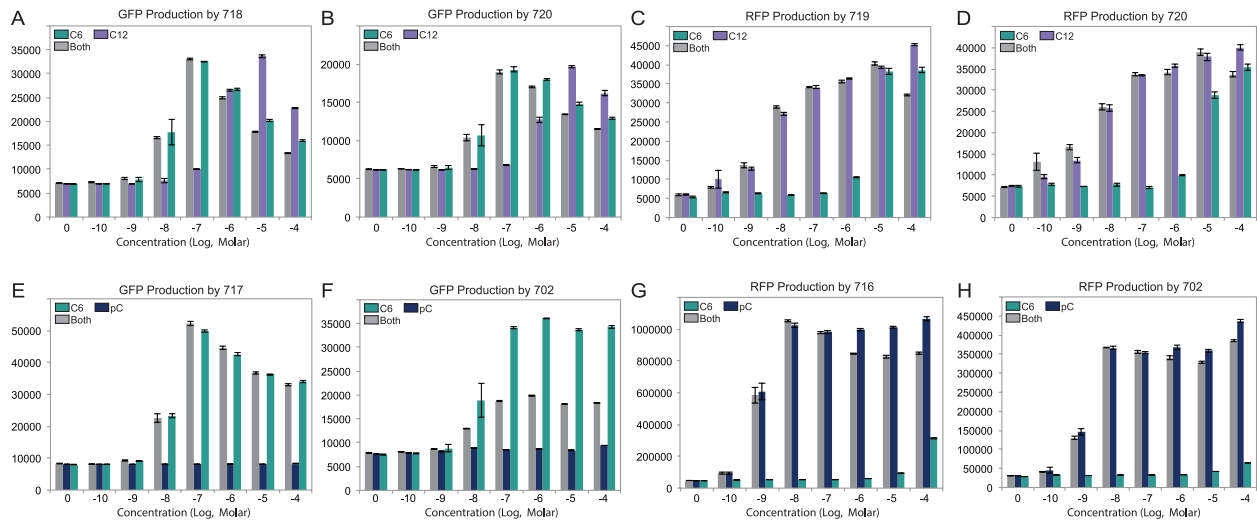


Fig. S5 Side-by-side comparison of raw fluorescence expression between 2-plasmid and 3-plasmid orthogonality strains. (A-D) Raw expression from promoter orthogonal strains 718, 717, and 720. (E-H) Raw expression from complete orthogonal strains 717, 716, and 702. Expression from Strain 717 with C6 and Both is almost identical, however from Strain 702, Both HSLs result in significantly less GFP which is likely a result of growth defects caused by metabolic load of producing RFP at the same time. Error bars represent S.E.M (n=4).

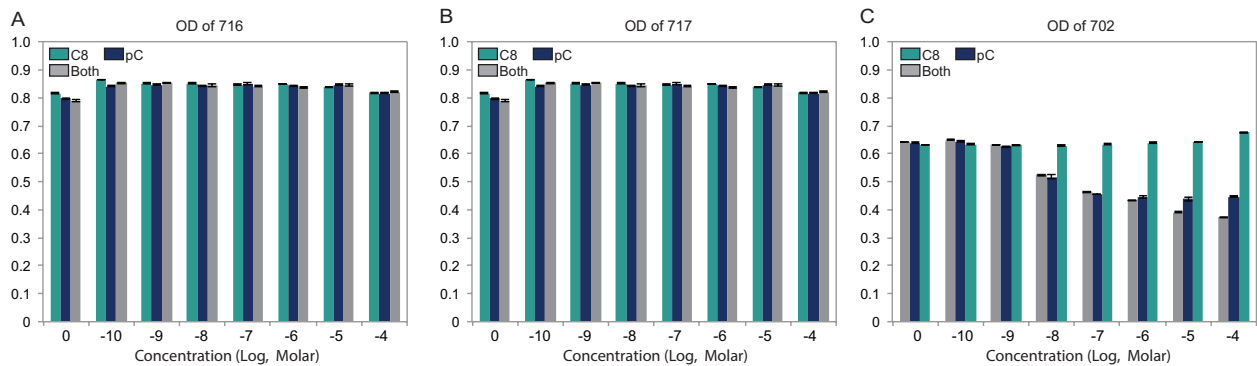


Fig. S6 Growth defects in the 3-plasmid “Complete Orthogonality” strain 702 compared to the 2-plasmid complete orthogonality strains of 716 and 717. (A-B) OD of strain 716 and 717 3 hours after induction with HSLs. No apparent change in OD due to HSL concentration. (C) Base level OD of Strain 702 is less, likely due to harboring three relative high-copy plasmids. Furthermore, OD decreases with increased concentrations of pC-HSL, likely due to growth defects caused by the production of RFP. These growth defects can distort the meaning of OD-normalized dose-responses. Error bars represent S.E.M (n=4).

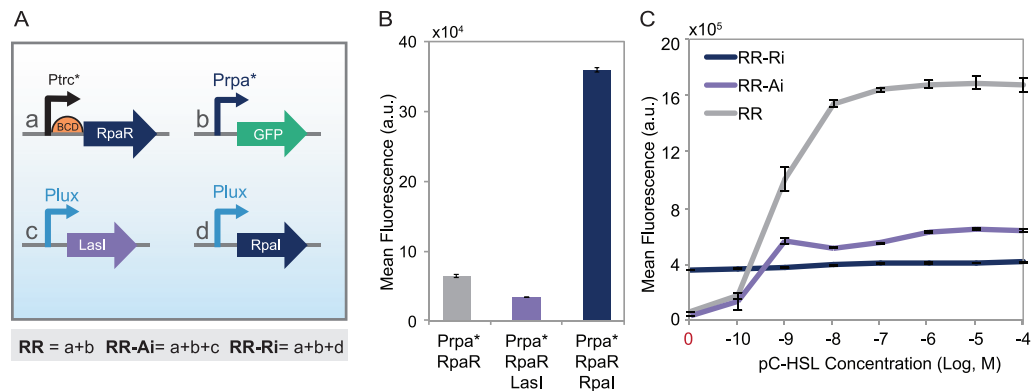


Fig. S7 Genetic circuit diagrams and fluorescence data. Panel A shows four genetic constructs: RR (a+b), RR-Ai (a+b+c), and RR-Ri (a+b+d). Panel B shows mean fluorescence for Prpa* RpaR, Prpa* RpaR Lasl, and Prpa* RpaR Rpal. Panel C shows mean fluorescence vs pC-HSL concentration for RR-Ri, RR-Ai, and RR.

Fig. S7 (B) Inclusion of an RpaI expressing plasmid causes increased GFP expression in an RpaR-expressing strain with GFP driven by the Prpa* promoter. Error bars represent S.D. (n=4). (C) Exogenously providing HSL to the strain with RpaI shows little induction at even the highest concentration of 100uM, hinting that RpaI alone saturates the production capabilities. Raw expression is likely less in the 3-plasmid systems for the same metabolic reasons previously described. Error bars represent S.D. (n=4).